Sub-50 nm positioning of organic compounds onto silicon oxide patterns fabricated by local oxidation nanolithography

N.S. Losilla,[a] N. S. Oxtoby,[b] J. Martinez,[a] F. Garcia,[a] , R. Garcia,[a,*] M. Mas-Torrent,[b] J. Veciana,[b] C. Rovira[b,*]

a) Instituto de Microelectrónica de Madrid, CSIC, Isaac Newton 8, 28760 Tres Cantos, Madrid, Spain
b) Instituto de Ciencia de Materiales de Barcelona, CSIC, Campus UAB, 08193 Bellaterra, Barcelona, Spain

We present a process to fabricate molecule-based nanostructures by merging a bottom-up interaction and a top-down nanolithography. Direct nanoscale positioning arises from the attractive electrostatic interactions between the molecules and silicon dioxide nanopatterns. Local oxidation nanolithography is used to fabricate silicon oxide domains with variable gap separations ranging from 40 nm to several microns in length. We demonstrate that a ionic tetrathiafulvalene (TTF) semiconductor can be directed from a macroscopic liquid solution (1μM) and selectively deposited onto predefined nanoscale regions of a 1 cm^2 silicon chip with an accuracy of 40 nm.

*Corresponding authors: rgarcia@imm.cnm.csic.es; cun@icmab.csic.es

Keywords: AFM, Nanolithography, Nanoparticles.

1. Introduction

Relatively inexpensive approaches for the fabrication of planar devices based on materials by design are critical for the development of organic-based electronics.[1-4] Taking advantage of several nanolithographies[5-7] as well as the self-organisation of functional molecules, it has been possible to fabricate surface patterns of these functional units with the proper position and shape and establish connections with other components of the device[8-12]. These approaches make use of specific interactions, such as hydrophobicity/hydrophilicity, electrostatic or protein recognition, between the components and the substrate. Organic semiconductors [13,14] are materials of particular importance as they are the active components in several electronic devices such as identification tags[15], electronic bar codes, electronic paper or active matrix elements for displays[16-17]. Tetrathiafulvalene (TTF) derivatives are in turn, remarkable semiconductors for preparing devices as Field Effect Transistors [18-22] and the obtained results already point out the high potential of these materials, which can be easily procesed [23] and tailored synthesized.[24] Even though nanostructuration of TTF derivatives in different surfaces has been demonstrated,[25-28] potential applications of TTFs as component in circuitry do still require methods for precise nanoscale controlled position and/or manipulation of those molecules.

We have applied a scanning probe microscopy-based lithography for controlling the positioning of the molecules. Local oxidation nanolithography is an atomic force microscopy (AFM) lithography technique that it is based on the spatial confinement of the oxidation reaction within a water meniscus formed between a nanometer-size

protrusion, usually the tip of an AFM and the sample surface [29-34]. The local oxidation process is rather stable and robust, and parallel upscaling of the nanolithography has been demonstrated by using a print-based approach.[35,36]. AFM nano-oxidation has been applied to fabricate a wide variety of templates for the growth of several organic and biomolecules such as oligothiophenes [7], single-molecule magnets[37], proteins[38,39] or gold nanoparticles[40-41].

Our present contribution is focused on the incorporation of organic semiconductors (TTF derivatives) onto silicon substrates based on the electrostatic interactions between charged TTF derivatives and the local oxide nanopatterns. We report a process for the transfer of charged TTF derivatives from a macroscopic liquid solution into a predetermined nanoscale region of a silicon surface. The method allows the fabrication of nanostructures made of TTF on silicon oxide templates separated 40 nm apart while the rest of the neighbourhood regions remain free of the molecules.

2. Experiments and discussion of results

We have synthesized the TTF derivatives **1** and **2** bearing polar charged groups (carboxylates) as substituents with different counterions that permit to solubilize the molecule either in water (sodium TTF salt **1**) or organic solvents (tetrabutylammoiun TTF salt **2**).[27] For comparison purposes, the neutral TTF derivative **3**[27] was also studied. The best results were obtained with the water soluble sodium salt **1** (figure 1).

A schematics of the process followed to position TTF molecules is presented in figure 2.

First, the silicon chip is immersed in a hot (80º C) $NH_4OH/H_2O_2/H_2O$ (1:1:10) solution for 15 minutes. This process removes the contaminants deposited on the substrate and leaves the surface with a very thin silicon dioxide (~0.6 nm). In the next step, a region of the surface is modified by local oxidation (figure 2(a)). Then a 20 μl drop of a sonicated 10^{-8} M solution of TTF **1** in H_2O, or TTF **2** and **3** in CH_2Cl_2, was deposited on the substrate (figure 2(b)) with deposition times varying between 10 s to one minute. Finally, after deposition, the substrate was rinsed in DI for a few seconds and blown dry in N_2 (figure 2(c)).

Nanoscale direct assembly arises from a combination of two factors: (i) the strength of the attractive electrostatic interactions between the molecules and the charged local oxides, (ii) the weak interaction between the molecules and the unpatterned surface.

The local oxidation of the silicon was performed with an amplitude modulation atomic force microscope operated in the low amplitude solution (noncontact or attractive regime) and with additional circuits to apply voltage pulses. The local oxidation experiments (water meniscus) were performed with the AFM exposed to the laboratory relative humidity (30-40%). As an example in figure 3, we show a SiO_2 pattern made of two pointed arrows separated above 220 nm.

The upper part of the pattern has been generated by the application of a voltage pulse of 24 V for 1 ms while the bottom part was generated by increasing the voltage to 30 V. The height of the local oxide depends on the strength and duration of the voltage [42]. The cross-section shows the top section with an average height of 0.8 nm while the bottom part has a height of 2.2 nm.

After the deposition of the TTF derivative **1**, we can observe in figure 4 that the molecules are mostly depositied on the bottom part. This is better appreciated by plotting dynamic force microscopy phase contrast images (figures 4(b) and (c)). The sensitivity of phase imaging to changes in energy dissipation processes [43] allows to achieve compositional contrast at the nanoscale without the interference of topography. The phase image allows us to visualize the different materials, silicon, nanooxide and nanoparticles. The experiment reveals that the compound **1** forms nanoparticles that are selectively deposited on the SiO_2 nanopatterns or at their edges with a precision below 40 nm (figure 4(c)). We also observe that the preferentiality of the interaction is substantially increased on the thicker nanopatterns. We have also deposited the non-charged TTF derivative benzodicarbomethoxy -tetrathiafulvalene **3**; however, here we did not observe any kind of preferential interaction between the local oxides and the molecules.

It is known that the local oxidation process, owing to the presence of very high electrical fields (1-10 V/nm), generates trapped ionic species [44]. The density of trapped charges depend on the total charged transfer between the electrolyte and the substrate, or in other words, on the height of the oxide.

We attribute the source of the preferential interactions between the TTF derivative **1** and local oxide nanopatterns to the electrostatic interaction of the molecules with the trapped charges generated inside the nano-oxide. The differences in the preferentiality observed between shallow and thick nano-oxides is attributed to the higher charge built-up obtained in the thicker nano-oxides. We hypothesized that the Na^+ cations remain tightly bounded to the TTF molecules during the deposition process and that dipole-dipole interactions are the driving force in the deposition process. These experiments also indicate the characteristic length scale of the weakly screened long range electrostatic forces generated by the trapped charges is of several micrometers because there are not nanoparticles around the SiO_2 nanopatterns. When the tetrabutylammonium salt **2** was used instead, the formation of nanoparticles were also observed, although the distribution size was not so homogenous in this case and, importantly, no preferential deposition on the local oxide nanopatterns was observed. This can be attributed to the loose character of the $TTF^{-}\ ^{+}NBu_4$ ion pair and that the formed assemblies are less polar [45].

The control achieved on the positioning of the organic semiconductor nanoparticles of **1** is demonstrated in figure 5.

We have fabricated several SiO_2 pointed arrows with a variable gap spacing between them. After the deposition of TTF **1**, the AFM images show that in all the patterns the molecules are located on top or at the edge of the patterns. No molecules are present in the gap between the nanopatterns and even the 40 nm gap is free of particles (figure 5(d)). This result emphasizes that the accuracy of the nanoscale deposition process is not affected

by the existence of nanopatterns separated by small gap distances; here the gap is about twice the average diameter of the nanoparticles. Furthemore, AFM images of the silicon surface in the neighborhood of the SiO_2 patterned region are free from molecules (figures 5(a) and (c)). The absence of molecules outside the patterned area emphasizes the selectivity of the positioning process.

AFM measurements of the deposited TTF **1** reveal an ellipsoidal-shaped morphology with an average height of 1 nm and an average width of 15 nm (full width at half maximum). The difference observed between height and diameter values (1 vs. 15 nm) is mostly due to tip's induced convolution [46]. It is widely known that tip-molecule convolution effects produces images of the molecules with an apparent diameter 2-5 times larger than its van der Waals value

One final point corresponds to when the nanoparticles are formed either in the solution or when deposited on the surface. For that purpose we have studied the carboxylate TTF derivative **1** in water solution by using Transmission Electron Microscopy (TEM), a technique which allows observation of the aggregates away from the surface, after depositing the compound from water solutions onto carbon coated copper grids. The samples were not coated with any contrast agent and the images were recorded at room temperature. The images clearly show that nanoparticles of the TTF sodium salt **1** are already formed in solution and have sizes that vary between 15-25 nm in agreement with AFM measurements. The observed sizes indicate that the nanoparticles are aggregates of several TTF derivative molecules. A representative example of the formed nanoparticles is shown in figure 6.

3. Conclusions

We have demonstrated a process for the nanoscale positioning of organic nanoparticles. The process is driven by the electrostatic interactions between the charged TTF derivative **1** and the charged SiO_2 nanopatterns. The main result is the transfer of a molecule from a macroscopic liquid volume to a nanoscale region of a patterned silicon surface with sub-50 nm accuracy. The accuracy of the positioning is dictated by the size of the lithography. The present process is scalable, allows multiple processing and requires inexpensive drop-casting deposition processes from liquid solution.

.

Acknowledgements. This work was supported by the European Commission under contract numbers G5RD-CT-2000-00349 and NAIMO integrated project no. NMP4-CT-2004-500355. Financial support from the DGI, MEC (Spain) (contract numbers MAT2006-03849 and CTQ2006-06333/BQU) and DGR, Catalonia (contract number 2005SGR00591) is also acknowledged.

References

[1] Facchetti A 2007 *Materials Today* **10** 28.

[2] Reese C, Bao Z 2007 *Materials Today* **10** 20.

[3] Stutzmann N, Friend R H, Sirringhaus H 2003 *Science* **299** 1881.

[4] Dinelli F,Murgia M, Cavallini M, Levy P, Biscarini F, De Leeuw D M 2004 *Phys. Rev. Lett.* **92** 116802.

[5] Sotomayor C M Torres 2003 *Kluwer Academic/Plenum Publishers, New York***.**

[6] Geissler M, Xia Y N 2004 *Advanced Materials* **16** 1249.

[7] Garcia R, Tello M, Moulin J F, Biscarini F 2004 *Nano Lett.* **4** 1115.

[8] Cui Y, Bjoerk M T, Liddle J A, Soennichsen C Boussert B Alivisatos A P 2004 *Nano Lett.*, **4** 1093.

[9] Barry C R, Gu J, Jacobs H O *Nano Lett.* 2005 **5** 2078.

[10] Lenhert S , Sun P, Wang Y H, Fuchs H, Mirkin C A 2007 *Small* **3** 71.

[11] Mesquida P, Stemmer A 2001 *Adv. Mater.* **13** 1395.

[12] Li D, Ouyang G,. McCann J T, Xia Y N 2005 *Nano Lett.* **5** 913.

[13] *Organic Electronics, materials, manufacturing and applications* Klauk H *Ed* 2006 *Wiley-VCH Verlag GmbH& Co. Weinheim***.**

[14] Forrest S R, Thompson M E 2007 *Chemical Reviews* **107** 923.

[15] Rotzoll R, Mohapatra S, Olariu V, Wenz R, Grigas M, Dimmler K, Shchekin O, Dodabalapur A 200**6** *Appl. Phys. Lett.* **88** 123502.

[16] Gelinck G H, Huitema H E A, van Veenendaal E, Cantatore E, Schrijnemakers L, van der Putten J, Geuns T C T, Beenhakkers M, Giesbers J, Huisman B H, Meijer E J, Benito E M, Touwslager F J,

Marsman A W, van Rens B J E, de Leeuw D M 2004 *Nat. Mater*. **3** 106.

[17] Lee S, Koo B, Park J G, Moon H, Hahn J, Kim J M 2006 *MRS Bull.* **31** 455.

[18] Mas-Torrent M, Durkut M, Hadley P, Ribas X, Rovira C 2004 *J. Am. Chem. Soc.* **126** 984.

[19] Mas-Torrent M, Hadley P, Bromley S T, Ribas X, Tarrés J, Mas M, Molins E, Veciana J, Rovira C 2004 *J. Am. Chem. Soc*. **126** 8546.

[20] Naraso, Nishida J I, Ando S, Yamaguchi J, Itaka K, Koinuma H, Tada H, Tokito S, Yamashita Y 2005 *J. Am. Chem. Soc*. **127** 10142.

[21] Mas-Torrent M, Rovira C 2006 *J. Mater. Chem.* **16** 433.

[22] Gao X K, Wu W P, Liu Y Q, Qiu W F, Sun X B, Yu G, Zhu D B 2006 *Chem. Comm.* 2750.

[23] Miskiewicz P, Mas-Torrent M, Jung J, Kotarba S, Glowacki I, Gomar-Nadal E, Amabilino D B, Veciana J, Krause B, Carbone D, Robira C, Ulanski J 2006 *Chem. Mater*. 4274.

[24] Yamada J-I, Sugimoto T 2005 *TTF Chemistry, Fundamentals and Applications of Tetrathiafulvalene*. Kodanska-Springer.

[25] Wang C, Zhang D, Zhu D 2005 *J. Am. Chem. Soc.* **127** 16372.

[26] Akutagawa T, Kakiuchi K, Hasegawa T, Noro S, Nakamura T, Hasegawa H, Mashiko S, Becher 2005 J *Angew. Chem. Int. Ed.* **44** 7283.

[27] Crivillers N, Mas-Torrent M., Bromley S. Wurst K, Veciana J, Rovira C 2007 *ChemPhysChem*; **8** 1565

[28] Puigmarti-Luis J, Minoia A, Uji-i H, Rovira C, Cornil J, De Feyter S, Lazzaroni R, Amabilino D B 2006 *J. Am. Chem. Soc*. **128** 12602.

[29] Garcia R, Martinez R V, Martinez J 2006 *Chemical Society Reviews* **35** 29.

[30] Xie X N, Chung H J, Sow C H, Wee A T S 2006 *Mat. Sci. Engin. R* **5** 1.

[31] Wouters D, Schubert U S 2004 *Angew. Chem. Int. Ed*. **43** 2480.

[32] Kinser C R, Schmitz M J, Hersam M C 2006 *Adv. Mater*. **18** 1377.

[33] Orians A, Clemons C B, Golovaty D, Young G W 2006 Surf. Sci. **600** 3297.

[34] Tseng A A, Notargiacomo A,Chen T P 2005 J. Vac. Sci. Technol. **23** 877.

[35] Martinez J, Losilla N S, Biscarini F, Schmidt G, BorzenkoT, Molenkamp LW, Garcia, R 2006 *Rev. Sci. Instrum.* **77** 086106.

[36] Hoeppener S, Maoz R, Sagiv J 2003 *Nano Lett.* **3** 761.

[37] Martinez R V, Garcia F, Garcia R, Coronado E, Forment-Aliaga A, Romero F M, Tatay S 2007 *Advanced Materials* **19** 291.

[38] Fresco Z M , Frechet J M J 2005 *J. Am. Chem. Soc*.**127** 8302.

[39] Yoshinobu T, Suzuki J, Kurooka H, Moon W C , Iwasaki H 2003 *Electrochimica Acta* **48** 3131.

[40] Chen C F,. Tzen S D, Lin M H, Gwo S 2006 *Langmuir* **22** 7819.

[41] Liu S, Maoz R, Sagiv J 2004 *Nano Lett*. **4** 845.

[42] Calleja M, Garcia R 2000 *Applied Physics Letters* **76** *3427.*

[43] Garcia R, Tamayo J, San Paulo A 1999 *Surf. Interf. Anal.* **27** 312.

[44] Dagata J A, Perez-Murano F, Martin C, Kuramochi H, Yokoama H 2004 *J. Appl. Phys.* **96** 2386.

[45] Zhu Q-Y, Lin H-H, Dai J, Bian G-Q, Zhang Y, Lu W 2006 *New J. Chem.* **30** 1140.

[46] Keller D 1991 *Surface Science* **253** 353.

Figure captions

Figure 1. Molecular formula of TTF derivative **1,2** and **3** used for the deposition onto predefined nanoscale regions of a silicon chip.

Figure 2. Schematics of the positioning of TTF derivatives. (a) Local oxidation of a region of the surface. (b) Deposition of a macroscopic drop of a solution containing polycationic TTF derivative (dark disks). (c) Rinsing removes the molecules from the unpatterned areas. Polycationic TTF derivative molecules are only attached to the nanopatterns.

Figure 3. Patterns fabricated by local oxidation nanolithography. (a) AFM topographic image of a nanopattern formed by two pointed arrows separated by a gap of 220 nm. The upper half of the pattern has been fabricated by applying a sequence of voltages pulses of 24 V for 1 ms, while the bottom part was generated by increasing the voltage to 30 V (t=1 ms). (b) Topographic AFM cross-section. The cross-section represents the average of the individual cross-section enclosed in the are marked in (a).

Figure 4. (a). AFM topographic image of the pattern shown in Fig. 2a after deposition of TTF derivative **1**. (b). AFM phase image of the left arrow shown in (a). (c). High resolution AFM phase image of the marked area in (b). TTF **1** is preferentially deposited on the thicker oxide section because the density of the trapped charges is higher in this region.

Figure 5. Positioning of TTF derivative **1** onto silicon oxide templates. (a) AFM topographic image of two pointed arrows after deposition of TTF **1**. The patterns are separated by a gap of 220 nm. (b) High resolution AFM topographic image of the region marked in (a). (c) The molecules appear as white dots in the image. (c). AFM topographic image of another pattern after the deposition of TTF derivative **1**. The patterns are separated by a gap of 40 nm. (d) High resolution AFM phase image of the region marked in (c).

Figure 6. TEM images of compound **1** after evaporation of the solvent from a 10^{-8} M solution of the sample in water on the holey carbon grid.

Figure 1

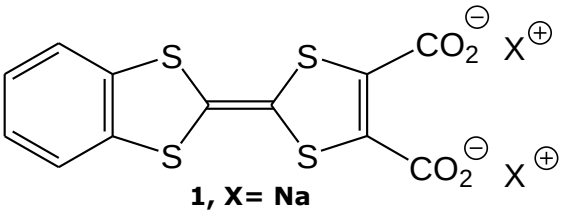

1, X= Na
2, X = NBu_4

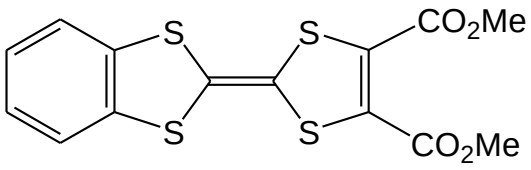

3

Figure 2

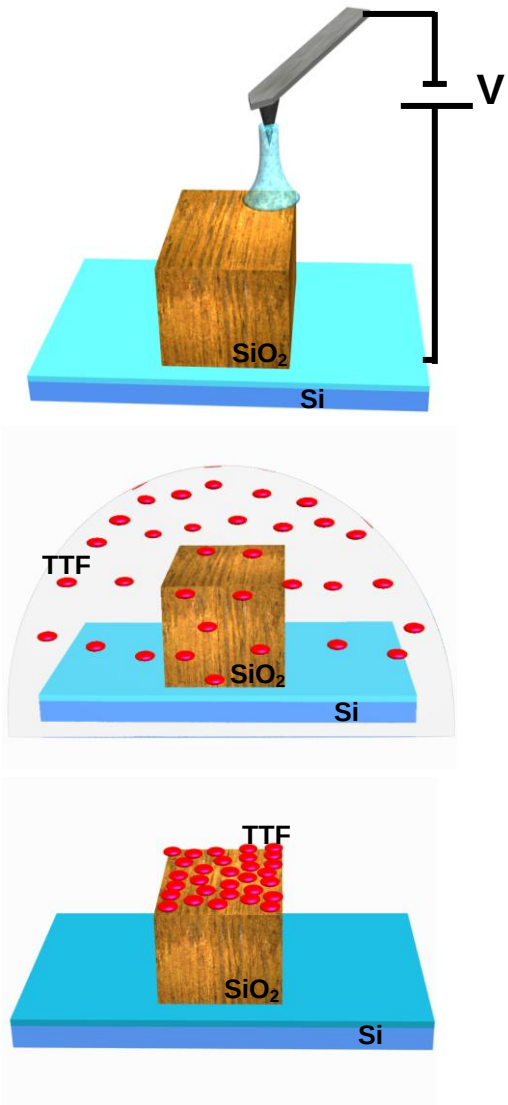

Figure 3

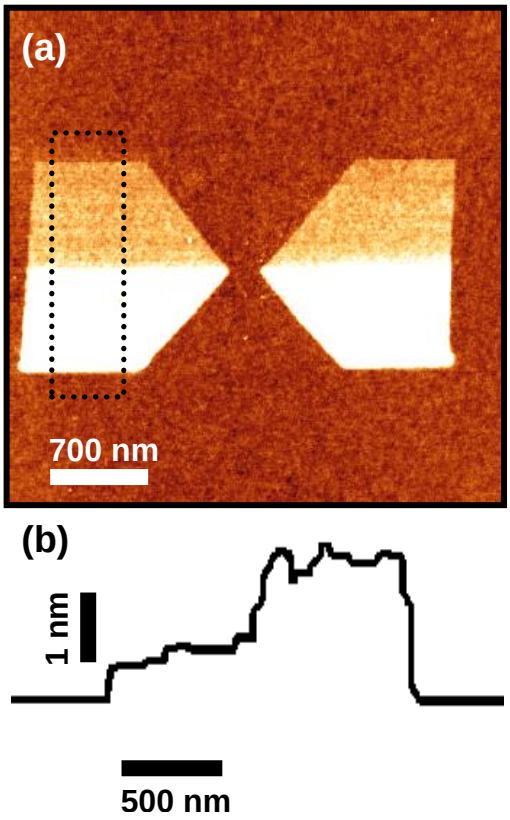

Figure 4

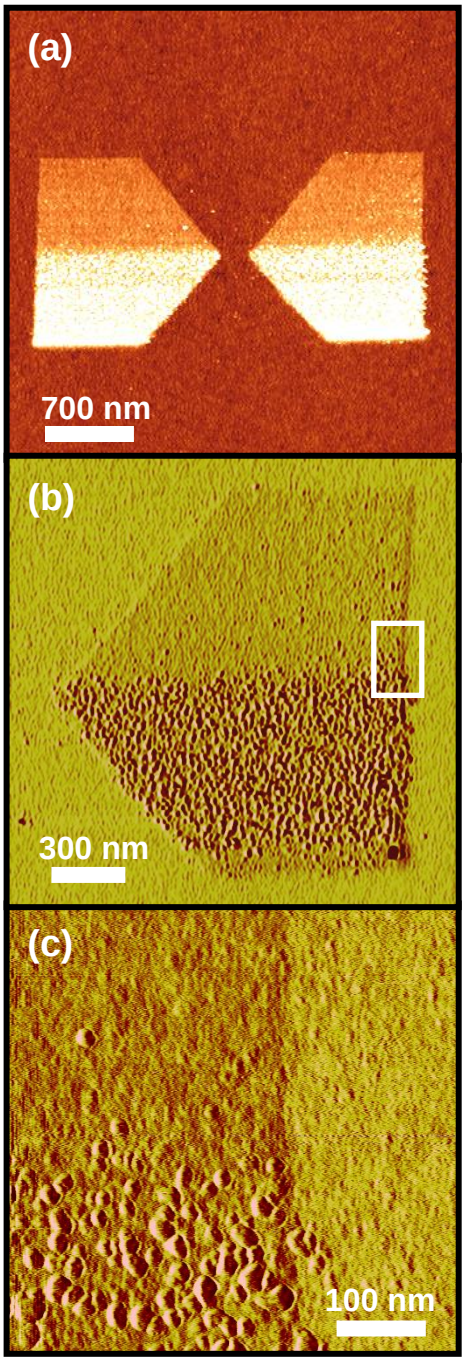

Figure 5

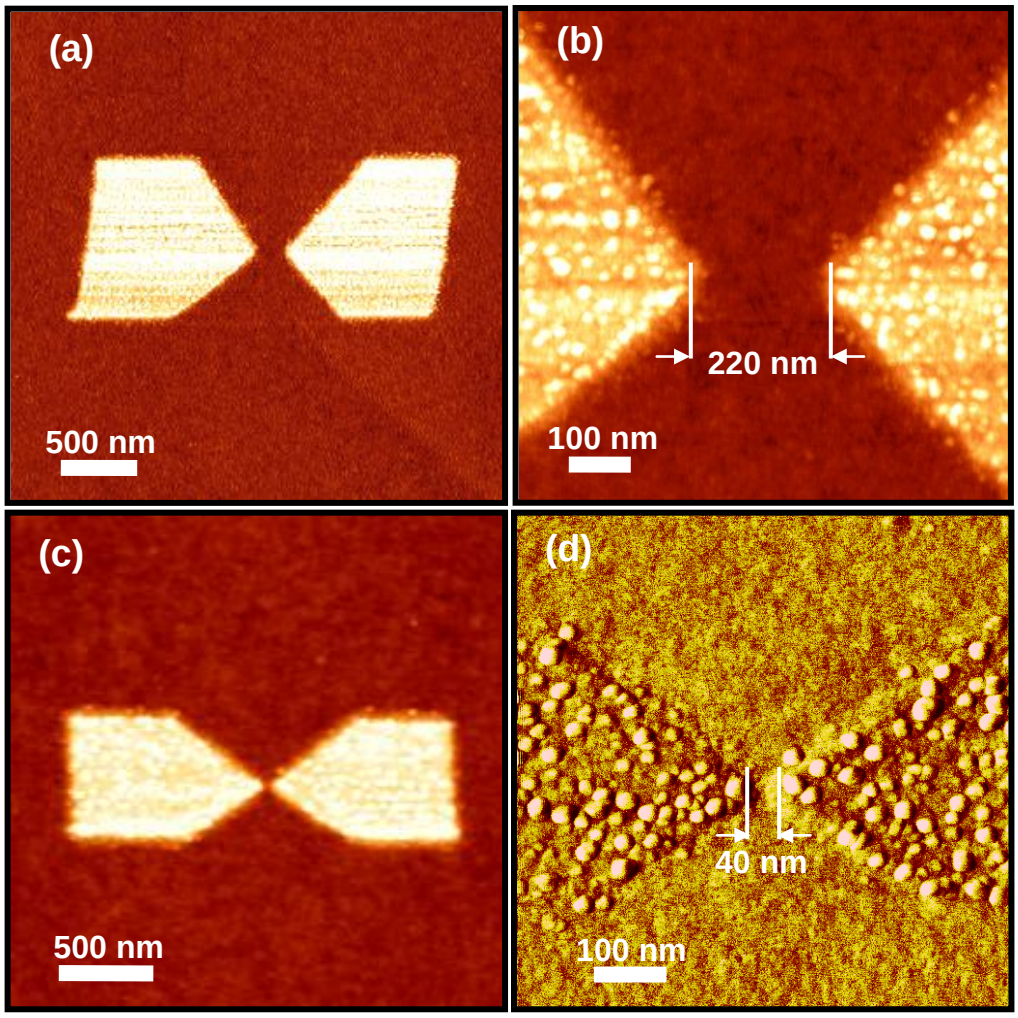

Figure 6